# Femtosecond Photoionization of Ion Beam Desorbed Aliphatic and Aromatic Amino Acids: Fragmentation via α-Cleavage Reactions

**Vasil Vorsa, Teiichiro Kono, Kenneth F. Willey,† and Nicholas Winograd***

*Department of Chemistry, The Pennsylvania State University, 184 Materials Research Institute Building, University Park, Pennsylvania 16802*

*Received: April 1, 1999; In Final Form: June 15, 1999*

We report the photoionization of ion beam desorbed amino acids using femtosecond laser pulses at 195 and 260 nm. Ionization of ion-desorbed glycine, alanine, valine, leucine, isoleucine, and phenylalanine using 195 nm laser pulses is found to produce almost exclusively a decarboxylated ion fragment, while tyrosine and tryptophan produce a functional group cation. The adiabatic ionization potentials for the former amino acids correspond to the removal of an electron from the amine nitrogen atom, while for tyrosine and tryptophan it corresponds to the removal of an electron from the aromatic functional group. We find that fragmentation is initiated by the formation of a radical site which leads to an α-cleavage reaction and, depending upon which electron is removed, results in the formation of a decarboxylated ion or a functional group ion. These results indicate that a significant fraction of the amino acids are desorbed intact, but are fragmented when ionized. Except for leucine, isoleucine, and phenylalanine, the mass spectra produced by 260 nm irradiation are similar to the mass spectra produced by 195 nm irradiation. When using these two wavelengths, the desorbed amino acids exhibit a 2- to 8-fold higher ion yield than is found using only secondary ions produced directly by the incident ion beam. Tyrosine exhibits up to a 40-fold increase in signal using 195 nm irradiation.

## Introduction

Many organic and biological molecules are thermally labile and do not volatize without significant decomposition. It is important in many areas of mass spectrometry to ionize these systems efficiently and at the same time to minimize fragmentation. While considerable progress has been made in ionizing large molecular systems intact using electrospray and matrix-assisted laser desorption ionization (MALDI), mass spectrometric surface characterization has been less successful in this regard. Early efforts have focused on using nanosecond lasers to photoionize neutral species desorbed from surfaces by either an energetic ion beam[1−6] or another laser beam.[7−10] This approach has been successful in increasing overall ion yields, particularly in atomic systems. However, in molecular systems, the advantages gained in increased ion yields are often offset by extensive photoinduced fragmentation.

The photophysical and photochemical behavior of molecules in the presence of ultrashort and intense laser fields is currently a topic generating considerable interest in mass spectrometry due to the extremely high optical pumping rates and unique ionization mechanisms.[11,12] Applications of high power femtosecond laser pulses are now emerging in areas of mass spectrometry and trace analysis.[13] Several reports suggest that the degree of fragmentation can be reduced considerably by using short laser pulses for ionization.[11,12,14−23] The potential for reducing fragmentation lies in increasing the laser intensity *dependent* rate of ionization over the intensity-*independent* rate of neutral fragmentation. In other words, the rate of dissociation from a dissociative state in the molecule is independent of the laser intensity. Since multiphoton ionization rates scale nonlinearly with laser intensity raised to the order of the photon process, the absorption rate under femtosecond excitation can be significantly increased over nanosecond excitation, particularly for nonresonant processes. One example of this dramatic increase in absorption rate for a nonresonant two-photon process is illustrated by Weinkauf et al.[11] for benzene where a 20-fold increase in molecular ion signal is observed using femtosecond excitation over nanosecond excitation while the laser pulse energies are kept equal. In addition to increasing signal levels for nonresonant excitation, a higher photon absorption rate also overcomes fast relaxation processes in intermediate states in resonant excitations. This is especially important in larger molecules, such as peptides, where several tens of electronvolts of energy can be stored in internal degrees of freedom. Currently, a considerable amount of work is underway in examining the efficacy of using ultrashort laser pulses to ionize various molecular systems intact.

Utilizing ultrashort laser pulses to reduce fragmentation and increase ion yields has considerable implications for many areas of surface characterization. One of these areas is the photoionization and subsequent detection of neutral species desorbed from surfaces following ion bombardment.[2,19] This technique is an extension of secondary ion mass spectrometry (SIMS) in which charged species resulting from the desorption event are analyzed directly with mass spectrometry. The fraction of charged sputtered particles turns out to be very small (<0.1%) for most cases. Thus, there is great potential in increasing ion yields (up to 3 orders of magnitude) by ionizing the neutral flux with laser ionization. Efficient detection is critical in these experiments since the primary ion dose needs to be kept at a minimum to avoid measurable damage to the surface.[24] Moreover, molecule-specific imaging experiments[1,25] are now placing even more stringent requirements on the detection of desorbed molecules. For these experiments, desorption occurs from a point on the surface of submicrometer size which contains less than $10^6$ molecules.

† Present address: Atom Sciences, Inc., 114 Ridgeway Center, Oak Ridge, TN 37830.

10.1021/jp991123c CCC: $18.00 
Published on Web 08/20/1999

Commercially available laser systems are presently capable of producing less than 100 fs pulses in the wavelength range from the near-IR to the UV with peak power densities up to $10^{15}$ W/cm$^2$.[16,26,27] The ionization mechanisms under these extreme laser conditions are currently the subject of much research.[12,28−32] In addition to low-order multiphoton processes that are normally operative under nanosecond laser conditions, high-order MPI processes such as above threshold ionization[28] become significant in the presence of higher laser intensities. Furthermore, at extremely high laser intensities, field ionization mechanisms such as tunnel and barrier suppression ionization are dominant.[12,29−32] These mechanisms could potentially give rise to ionization techniques that produce little or no fragmentation in addition to higher ion yields. Presently, however, many molecules are still observed to undergo extensive fragmentation even when interacting with ultrashort pulses, and especially when the power density is increased to achieve maximum ionization efficiency.[16,33]

In this paper, we examine the behavior of ion-desorbed aliphatic and aromatic amino acids following ionization with UV femtosecond laser pulses. Amino acids have a common backbone consisting of $COOHCHNH_2$ in which ionization can take place through the nitrogen atom. Moreover, in aromatic amino acids the functional groups provide an additional point for ionization. Preliminary experiments on these amino acids with femtosecond laser pulses showed there is considerable fragmentation.[16] To determine the mechanism of fragmentation we have examined the photoionization mass spectra of the aliphatic and aromatic amino acids resulting from 260 and 195 nm photon irradiation. The results strongly suggest that the amino acids are desorbed and ionized intact but then subsequently fragment via radical cleavage reactions. A mechanism is proposed which illustrates that the fragmentation pattern is dependent upon which electron is removed from the amino acid. Finally, we compare ion yields and fragmentation to those observed with SIMS.

## Experimental Techniques

The amino acid samples were purchased from Sigma and used without further purification. Each amino acid was dissolved to a concentration of $\sim 10^{-2}$ M in a 50/50 solution of HPLC grade water and absolute ethanol. The solution was then pipetted onto a clean Si wafer and allowed to dry before analysis. The TOF-SIMS instrument has been described in detail previously.[25] Briefly, high-energy (25 keV) $Ga^+$ ions produced by a liquid metal ion gun (LMIG) (Ionoptika) are directed at the sample, inducing desorption of ion and neutral species. The sample block is cooled to $-125°$ C in order to reduce the background signal caused by sublimation of the sample.[1] For SIMS experiments, the secondary ions formed at the sample surface are pulse extracted into a dual-field reflectron TOF mass analyzer by applying a positive potential (2.5 kV) directly to the sample stage. For laser ionization experiments, charged particles produced at the surface are suppressed by setting the sample stage to a negative potential prior to laser ionization. Neutral species intersect the laser beam at a distance of 100−200 $\mu$m above the surface. The ensuing photoions are accelerated with a pulsed positive potential into the reflectron mass analyzer where they are separated according to mass and detected by a dual microchannel plate detector. Signal levels for all the experiments presented here were in the single ion counting regime. Each ion pulse is sent through a $\times 4$ preamplifier and a discriminator. The output of the discriminator is sent to a time-to-digital converter (model 9805, Precision Instruments Inc.) with 1 ns time resolution. This reflectron mass analyzer yields a mass resolution of 1 part in 3000 in the range $m/z = 20-300$.

The Ti:sapphire femtosecond laser system (Clark-MXR, Inc.) employed in these experiments has been described previously.[15,16] Briefly, the output of a self-mode-locked Ti:sapphire oscillator pumped by an $Ar^+$ laser (Spectra Physics) used to seed a Ti:sapphire regenerative amplifier using chirped pulse amplification techniques. The final output from the system is a 1 kHz train of pulses at 780 nm and containing $\approx$3.5 mJ of energy per pulse at a pulse width of $\approx$100 fs. The 780 nm output is sent directly into a harmonic generator to produce additional wavelengths at 260 and 195 nm. An upper limit of 230 and 400 fs was measured for the 260 and 195 nm beam, respectively, by cross-correlation.[16] The laser is coupled into the analysis chamber with a 25 cm focal length $CaF_2$ lens. The laser spot size and position over the sample is controlled by movement of this lens mounted on an *x*, *y*, *z* manipulator outside the chamber. By changing the laser pulse energy and focal dimensions, the laser power density (measured in W/cm$^2$) in the extraction region may be varied over several orders of magnitude.[15]

## Multiphoton Ionization

Molecular fragmentation during multiphoton ionization can result from one of two distinct pathways. First, suppose a molecule is irradiated by a relatively long laser pulse from a nanosecond laser and is excited to a dissociative state. This molecule will most likely dissociate because the rate of multiphoton absorption is generally orders of magnitude slower than the rate of dissociation (assuming direct dissociation) due to the relatively low laser intensities of nanosecond lasers.[11] Moreover, because the time scale for dissociation is orders of magnitude shorter than the laser pulse width, the fragments can absorb additional photons and undergo ionization themselves. In this case, dissociation precedes ionization and falls under the multiphoton model termed ladder switching.[11,14] On the other hand, if no dissociative state of the neutral molecule is excited during absorption or if the state leading to dissociation is a long-lived state, then the ionization level can be reached before dissociation occurs in the neutral molecule. Moreover, following ionization, it is possible that additional photons can be absorbed leading to dissociation. This is generally known as ladder climbing.[11,14] The cross section of absorbing additional photons by ions is enhanced due to the much higher density of electronic states in ions. Ladder climbing and ladder switching are illustrated in Figure 1. In addition to dissociation caused by the absorption of additional photons, the initial excited state of the ion may itself be dissociative. Fragmentation that occurs following ionization is known as ionization followed by dissociation.

To avoid possible fragmentation from ladder switching, ionization using ultrashort ($<$1 ps) laser pulses has been applied. Since the rate of dissociation $W_d$ for a particular state, once it is reached, is independent of the laser intensity, the only way to avoid dissociation is to increase the intensity-dependent rate of ionization $W_i(I)$ by increasing the laser intensity $I$. This can be achieved by decreasing the laser pulse width and thus increasing the laser intensity so that the absorption rate becomes greater than the intensity-independent dissociation rate (see Figure 1). Moreover, decreasing the laser pulse width reduces the potential of ionizing any fragments that may have been formed.

In addition to MPI, field ionization can also become important when using ultrashort amplified laser pulses.[28] During field

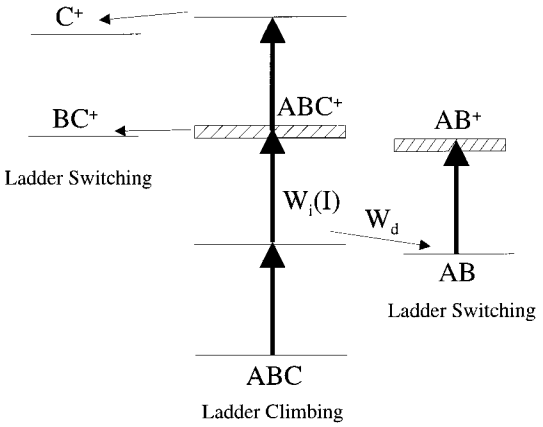


**Figure 1.** Illustration of two distinct dissociation pathways that can result during multiphoton ionization. First, dissociation can originate in a neutral state of the molecule whose fragments can, in turn, absorb additional photons leading to ionized fragment ions (ladder switching). The rate of dissociation $W_d$ from this state is independent of laser intensity. Conversely, an intact parent ion can be formed first followed by direct dissociation from either the initial ion state or by absorbing additional photons (ladder climbing). Under multiphoton conditions, neutral dissociation will compete with direct ionization. Increasing the laser intensity increases the ionization rate $W_i(I)$ while leaving the dissociation rate $W_d$ unchanged.

ionization, the electric field is comparable to or greater than the Coulombic field between the valence electron and the nucleus. In this case, the electron has the potential to escape via barrier suppression or tunnel ionization. A simple calculation employing the Keldysh parameter[33,34] suggests that the laser intensities used here are well below the field ionization regime of $10^{14}$ W/cm$^2$.

## Results and Discussion

Here we examine the photoionization of aliphatic and aromatic amino acids with UV femtosecond laser pulses following ion beam induced desorption. Fragmentation patterns from the mass spectra are compared as a function of the amino acid R-group and wavelength. First, 195 nm photoionization patterns are presented for the two groups of amino acids to determine the origin of fragmentation. For all amino acids studied here, the 195 nm photoionization produces relatively simple mass spectra. Next, the 260 nm results are presented to provide additional clues into the fragmentation patterns. Finally, the photoionization mass spectra and ion yields are compared with SIMS.

**195 nm Photoionization.** The 195 nm photoionization mass spectra of glycine, alanine, valine, leucine, and isoleucine are shown in Figure 2. None of these aliphatic amino acids have significant absorption above 200 nm, and the first absorption band arises from a n $\rightarrow \pi^*$ excitation in the amino group around 195 nm.[35] Immediately evident is the elimination of the carboxyl group moiety from the amino acids with little other fragmentation, thus indicating that all of these fragments arise from similar precursors and that they each ionize with a similar photoionization mechanism. Moreover, essentially no molecular ion is observed in any of the spectra. At relatively low laser power densities, the decarboxylated fragment ions dominate the mass spectra. Only at very high laser power densities ($>10^{11}$ W/cm$^2$) do the spectra exhibit considerable fragmentation into other channels.

The 195 nm photoionization mass spectra of the aromatic amino acids taken at near threshold power densities are shown in Figure 3. The base peak in the phenylalanine mass spectrum

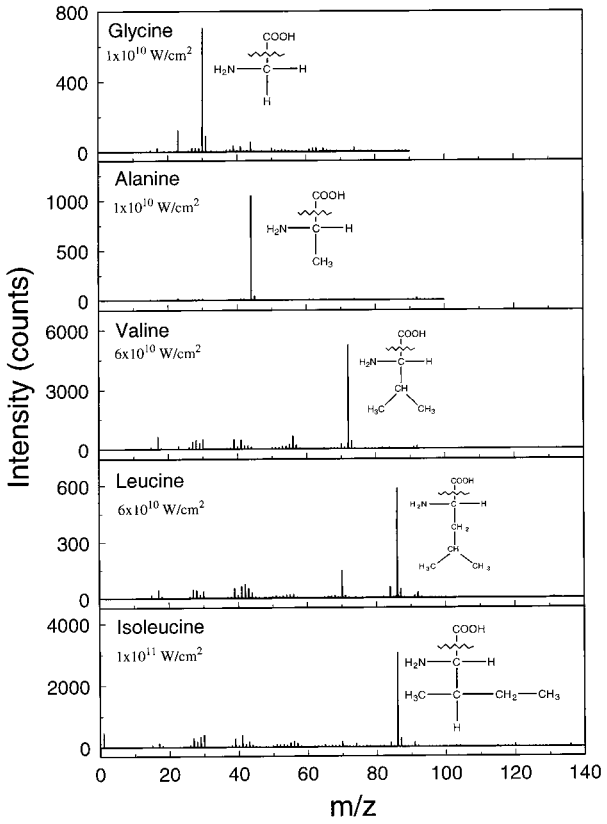


**Figure 2.** Femtosecond ionization mass spectra of ion-desorbed glycine, alanine, valine, leucine, and isoleucine with 195 nm excitation.

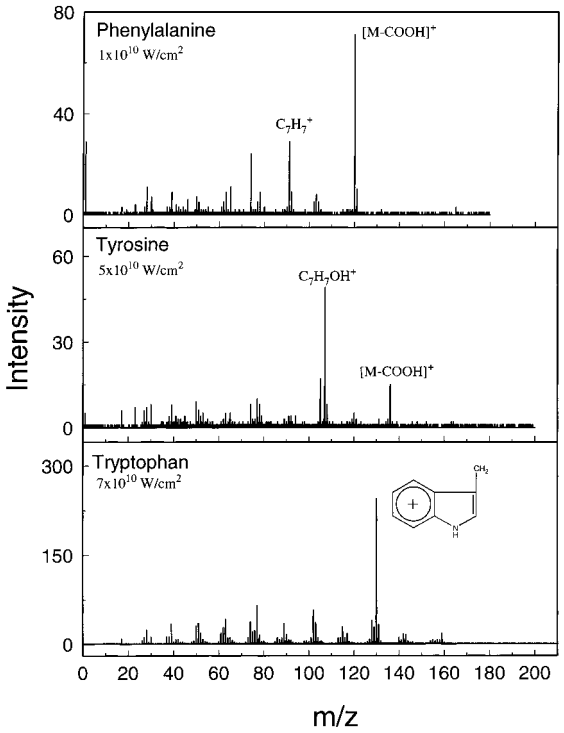


**Figure 3.** Femtosecond ionization mass spectra of ion-desorbed phenylalanine, tyrosine, and tryptophan with 195 nm excitation.

corresponds to the elimination of the carboxyl group. In addition to the decarboxylated amino acid, the $C_7H_7^+$ ion and the amino acid backbone $COOHCHNH_2^+$ are observed at *m*/*z* 91 and 74, respectively. These latter two fragments rapidly dominate the mass spectrum at higher laser power densities, indicating that they arise from a higher order photon process.[16] Structurally,

**TABLE 1: Lowest Adiabatic and Nitrogen Lone Pair Ionization Energies for the Amino Acids Studied Here[48]**

| amino acid | first IP[a] | N IP[b] |
|---|---|---|
| Gly | 8.8 | 8.8 |
| Ala | 8.9 | 8.9 |
| Val | 8.7 | 8.7 |
| Leu | 8.5 | 8.5 |
| Ile | 8.7 | 8.7 |
| Phe | 8.5 | 8.5 |
| Tyr | 8.0 | 8.6 |
| Trp | 7.2 | 8.7 |

[a] Lowest adiabatic IP in electronvolts. [b] Nitrogen lone pair IP in electronvolts.

tyrosine and phenylalanine are the same except for an additional hydroxyl group on the phenyl ring in tyrosine. However, the 195 nm fragmentation pattern of tyrosine differs considerably. The base peak in the tyrosine mass spectrum results from the elimination of the amino acid backbone producing the functional group moiety $C_7H_7OH^+$ at *m*/*z* 107. A smaller fragment peak is also observed which arises from the loss of the carboxyl group. Similar to tyrosine, the base peak in the tryptophan mass spectrum also arises from the elimination of the amino acid backbone resulting in the formation of a dehydroindole ion at *m*/*z* 130. However, unlike tyrosine, tryptophan does not exhibit a significant amount of fragment ions corresponding to loss of the carboxyl group.

To determine the likely fragmentation mechanism, it is useful to consider the ionization potentials of the amino acids. Listed in Table 1 are the adiabatic ionization energies and nitrogen lone pair ionization energies of the amino acids studied here. Ionization of these amino acids requires the absorption of at least two photons at 195 nm. The lowest adiabatic ionization energies of all the amino acids except tyrosine and tryptophan correspond to the removal of one of the lone pair electrons from the nitrogen atom. For tyrosine and tryptophan, the lowest adiabatic ionization energy corresponds to the removal of an electron from the aromatic functional group. Further examination reveals a correlation between the fragmentation pattern and the subgroup responsible for ionization. For amino acids in which the adiabatic ionization potential corresponds to the removal of an electron from the nitrogen atom, we observe the elimination of the carboxyl group. Conversely, for amino acids in which the adiabatic ionization potential corresponds to the removal of a functional group electron, we observe the formation of a functional group ion. This correlation between the adiabatic ionization potential and mass spectral patterns indicates that fragmentation is mediated by the location of the positive charge in the molecule. α-Cleavage is a dominant reaction mechanism in amines stemming from the nitrogen atom's electron donating ability.[36] This is illustrated for amino acids as

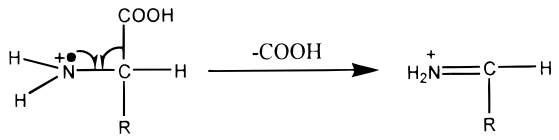


The radical site on the nitrogen atom initiates the reaction by donating an electron in the formation of a double bond between the nitrogen and carbon atoms. The second electron is donated from the carbon−carboxyl bond, thus cleaving the bond and generating a carboxyl radical.

The adiabatic ionization potentials of tyrosine and tryptophan correspond to the removal of an electron from the aromatic functional group of the amino acid instead of the removal of a nitrogen lone pair electron. The dominant ions observed for these two amino acids are the functional group moieties. Analogous to aliphatic amino acids, these ions likely arise from an α-cleavage reaction, but one which originates in the functional group rather than in the amine. α-Cleavage is commonly observed in aromatic hydrocarbons upon ionization.[33,36] In tyrosine and tryptophan, a radical site is formed in the ring, which initiates the reaction. For tyrosine, this reaction proceeds as

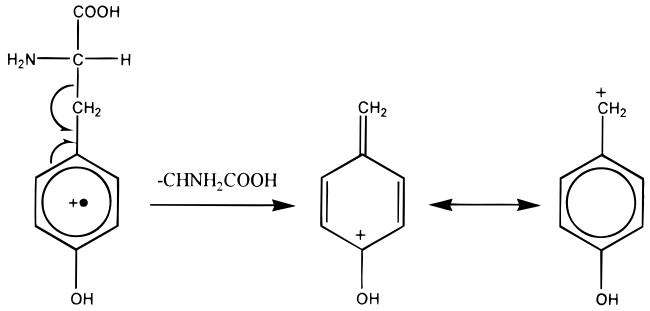


For fragmentation to proceed via the above mechanisms, the amino acid must be desorbed from the surface intact.

While fragmentation due to the desorption step followed by photoionization cannot be ruled out completely, the correlation between the fragmentation patterns and adiabatic ionization potentials suggests that a large number of the observed ions originate from intact amino acids. To gain further insight into the origin of these fragment ions, we performed photoionization experiments at 195 nm on gas-phase aromatic amino acids, which were thermally desorbed into the gas phase in the same manner as previously reported for dopamine.[33] At comparable laser power densities, the photoionization mass spectra of these gas-phase amino acids are remarkably similar to the ion-desorbed mass spectra with essentially no molecular ions produced. The similarity in the fragmentation patterns and the absence of molecular ions further indicates that large numbers of neutral amino acids are likely desorbed from the surface intact with fragmentation following ionization.

**260 nm Photoionization.** The first electronic absorption band (∼195 nm) of the aliphatic amino acids studied here results from a $n \rightarrow \pi^*$ excitation of a lone pair electron on the nitrogen atom.[35] On the other hand, a $\pi \rightarrow \pi^*$ excitation in the functional group of aromatic amino acids leads to a broad absorption feature between 250 and 280 nm.[35] To gain further understanding of the photoionization mechanism, spectra were acquired with 260 nm excitation. The photoionization mass spectra of the aliphatic amino acids following 260 nm excitation are shown in Figure 4. Except for glycine and alanine, the 260 nm mass spectra differ from those taken with 195 nm, particularly in the degree of fragmentation, which appears to increase with increasing side chain length. This is somewhat surprising since two-photon ionization with 260 nm (9.3 eV) is considerably less energetic than two-photon ionization with 195 nm (12.4 eV). Most significantly, leucine and isoleucine do not exhibit fragment ions corresponding to decarboxylation. However, these two amino acids do exhibit a fragment ion corresponding to the loss of both the carboxyl and amine groups. The valine mass spectrum is similar to glycine and alanine in that the largest peak is the decarboxylated ion, but it differs by exhibiting more fragmentation. Qualitatively, these spectra do not change significantly even at near threshold laser intensities. At this point, it is not clear what leads to more extensive fragmentation using 260 nm excitation. The adiabatic ionization potentials for these

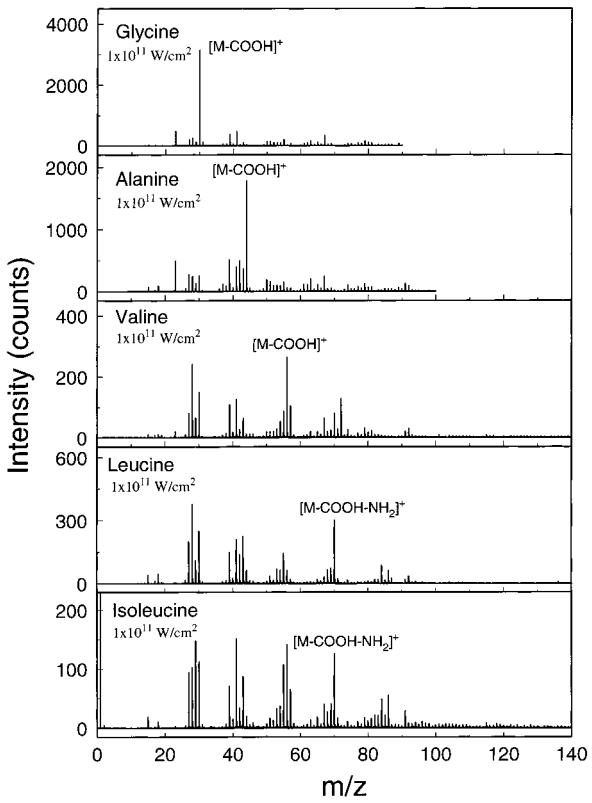


**Figure 4.** Femtosecond ionization mass spectra of ion-desorbed glycine, alanine, valine, leucine, and isoleucine with 260 nm excitation.

amino acids range from 8.5 to 8.9 eV. Depending upon the amino acid, absorption of two 260 nm photons deposits 0.4−0.8 eV of additional energy into the system (internal + electron kinetic energy). This is substantially less energy than the absorption of two 195 nm photons (12.4 eV). It is possible that an electron other than a nitrogen lone pair electron is removed in leucine and isoleucine, thus causing a different fragmentation pattern.

Mass spectra of the aromatic amino acids taken at a wavelength of 260 nm are shown in Figure 5. The 260 nm mass spectra of tyrosine and tryptophan are similar to those acquired with 195 nm in that the functional group ion is the dominant peak. These fragments arise from an α-cleavage of the C−C bond on the functional group, which is initiated by removing an electron from the ring. However, like the larger aliphatic amino acids, 260 nm excitation also generates an additional fragment peak corresponding to the loss of both the carboxyl and amine groups. This is not observed for any of the amino acids excited with 195 nm. The mass spectrum of phenylalanine taken with 260 nm, on the other hand, does not resemble the 195 nm spectrum. Excitation of phenylalanine at 260 nm results predominantly in the generation of the $C_7H_7^+$ fragment ion, similar to the $C_7H_7OH^+$ ion generated by tyrosine. Removal of a $\pi$-electron from the aromatic ring rather than a lone pair electron from the amine will result in the formation of $C_7H_7^+$, even though the ionization energy for this electron is greater. Due to the strong absorption cross section of phenylalanine, which peaks around 270 nm, it is possible that ionization through the phenyl group dominates over the removal of an amine electron at this wavelength. A higher photon order processes for generating $C_7H_7^+$ was also considered; however, power dependence data show this product to be dominant even at low laser power densities. Gas-phase photoionization mass spectra of the aromatic amino acids were also taken at 260 nm with comparable laser power densities to those used in the ion

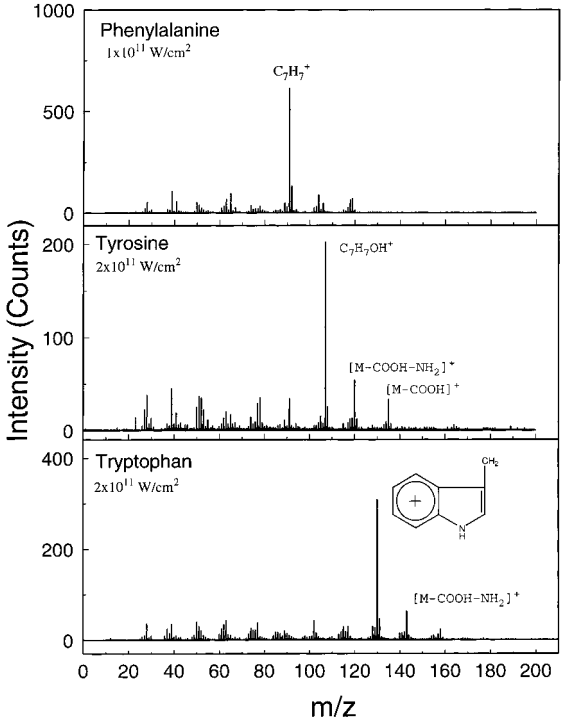


**Figure 5.** Femtosecond ionization mass spectra of ion-desorbed phenylalanine, tyrosine, and tryptophan with 260 nm excitation.

desorption experiments. Like the 195 nm gas-phase mass spectra, the 260 nm fragment ion mass spectra of tyrosine and tryptophan are generally similar to the ion-desorbed spectra with the exception that tyrosine also exhibits a substantial molecular ion peak comparable in intensity to the functional group ion. Phenylalanine, however, exhibits a different fragmentation pattern at 260 nm. In fact the dominant peak in this spectrum is the decarboxylated ion rather than the functional group ion. It is not apparent at this point why phenylalanine exhibits this differing behavior. However, the general correlation between the fragmentation patterns of the ion-desorbed and gas-phase species indicate that a significant fraction of the amino acids are not fragmented prior to photoionization, but rather they are intact with fragmentation following ionization.

It should also be mentioned, at this point, that the degree of vibrational excitation in the amino acids does likely effect the extent of fragmentation. For example, in laser desorption followed by laser ionization (LDLI) experiments using jet-cooling, [37] mass spectra taken with nanosecond lasers pulses at 266 nm result in predominantly parent ion formation for tyrosine and phenylalanine with some fragmentation into the functional group and decarboxylated ions, respectively. Tryptophan, while it does exhibit greater fragmentation, still generates a significant (40%) molecular ion signal. The lack of molecular ion signal in the ion desorption experiments may possibly be caused by concomitant vibrational excitation induced by the desorption event. Fragmentation resulting from excited electronic states is ruled out because ionization from an excited electronic state would exhibit a one-photon power dependence at 195 and 260 nm, which we do not observe.

Charge localization dependent fragmentation has been previously observed in gas-phase peptides by Weinkauf et al.[38] In these experiments, small peptides were ionized through a terminal tyrosine. Intramolecular charge transfer of the positive charge from the tyrosine to a terminal alanine was then initiated via photoexcitation leading to the formation of an immonium fragment ion by dissociation of the carboxyl bond. It is possible

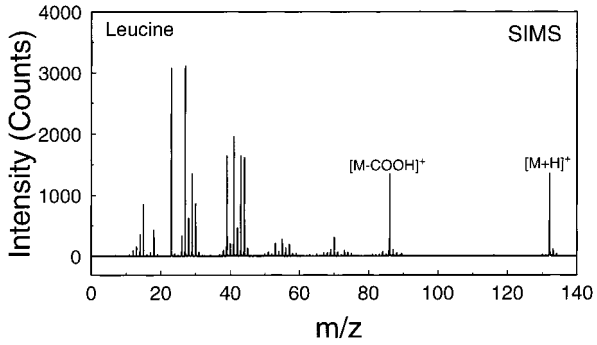


**Figure 6.** TOF-SIMS spectrum of leucine.

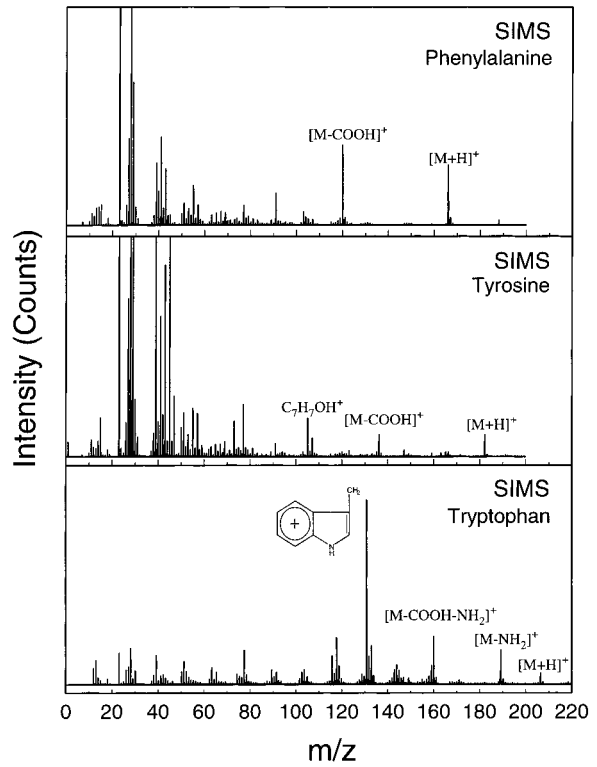


**Figure 7.** TOF-SIMS spectra of phenylalanine, tyrosine, and tryptophan.

that similar intramolecular charge transfer could be taking place here as well since the energy of two photons at either 260 or 195 nm is substantially greater than the two sets of ionization energies.

**Photoionization versus SIMS Ion Yields.** Here we make a direct comparison of the photoionization mass spectrum of ion-desorbed amino acids with the corresponding SIMS spectrum. The SIMS mass spectra we obtain are similar to previously reported amino acid mass spectra.[24,39−42] All the aliphatic amino acid SIMS mass spectra exhibit the formation of the quasimolecular ion $(M + H)^+$ and decarboxylated ion $(M - COOH)^+$. These two ions are also commonly observed in laser desorption mass spectrometry of amino acids.[43−47] The quasimolecular ion is stabilized by the additional proton which removes the radical site on the amine in addition to providing a positive charge. The positive ion SIMS spectrum of leucine is shown in Figure 6. Two major ion peaks characteristic of leucine are found at $m/z = 132$ $(M + H)^+$ and 86 $(M - COOH)^+$ with approximately equal intensity. The positive ion SIMS mass spectra of the aromatic amino acids are shown in Figure 7. Phenylalanine is similar to the aliphatic amino acids exhibiting the quasimolecular ion at *m*/*z* 166 and the decarboxylated ion at *m*/*z* 120. The tyrosine mass spectrum contains the quasimolecular ion, decarboxylated ion, and functional group ion. The dehydroindole ion is the dominant peak in the SIMS mass spectra of tryptophan. In addition, the quasimolecular ion *m*/*z* 205, the molecular ion minus the amine *m*/*z* 188, and the molecular ion minus the amine and carboxyl *m*/*z* 159 are also observed, but with lower intensity.

**TABLE 2: Absolute Ion Yields in Ion Counts for Each Characteristic Ion Channel Obtained with SIMS 260 and 195 nm Photoionization[a]**

| amino acid | SIMS | 260 nm | 195 nm |
|---|---|---|---|
| Gly | 8500 | 72600 (8.5) | 41900 (4.9) |
| Ala | 13900 | 72900 (5.2) | 63800 (4.6) |
| Val | 23200 | 40700 (1.8) | 86100 (3.7) |
| Leu | 12000 | 28500 (2.4) | 31300 (2.6) |
| Ile | 13900 | 17900 (1.3) | 29600 (2.1) |
| Phe | 6600 | 35500 (5.4) | 24300 (3.7) |
| Tyr | 1100 | 37400 (34) | 45400 (41) |
| Trp | 6600 | 42300 (6.4) | 29000 (4.4) |

[a] Increases in signal levels for 260 and 195 nm over SIMS are given in parenthesis for each amino acid. The data were collected under identical ion dose conditions.

In addition to comparing mass spectra, it is useful for analytical purposes to compare total ion yields formed by SIMS and photoionization. The total number of ions generated with laser ionization generally exceeds that observed for SIMS. A comparison of the absolute ion yields for identical ion bombardment conditions is shown in Table 2. These results are achieved by positioning the laser beam ~250 $\mu$m above the sample surface and focusing the laser beam to a spot size between 50 and 200 $\mu$m. The ion yields were calculated by summing all the molecular (quasimolecular) and characteristic fragment ions yields for each amino acid. The characteristic ions are identified in the above text and in the figures. The total characteristic ion yield for most of the amino acids is 2- to 8-fold higher for laser ionization than for SIMS, while tyrosine exhibits a 40-fold increase in signal with 195 nm ionization.

## Conclusions

Femtosecond photoionization studies of several ion beam desorbed aliphatic and aromatic amino acids have been carried out at wavelengths of 195 and 260 nm. No molecular ions are observed for any of the amino acids studied here at either wavelength. The dominant fragment channel for the five aliphatic amino acids and phenylalanine at 195 nm is decarboxylation. Moreover, the 195 nm mass spectra of the five aliphatic amino acids are particularly uncluttered. The major ion peak in the 195 nm photoionization mass spectra of tyrosine and tryptophan is the functional group moiety. The fragmentation patterns exhibit a correlation with the amino acid adiabatic ionization potential and are consistent with $\alpha$-cleavage reactions initiating at the sight of the lowest adiabatic ionization potential on the molecule. The five aliphatic amino acids and phenylalanine have adiabatic ionization potentials that correspond to the removal of a nitrogen lone pair electron, while for tyrosine and tryptophan they correspond to the removal of a $\pi$-electron from the functional group. The data suggest that a large fraction of the amino acids are desorbed from the surface intact and that fragmentation occurs after the molecules have been ionized. Ionization with 260 nm produces similar results for all the amino acids except for leucine and isoleucine, which exhibit extensive fragmentation and essentially no ion fragments corresponding to decarboxylation, and phenylalanine which yields a functional group ion. The reason that the fragmentation pattern deviates

for phenylalanine at 260 nm is not clear at this point, but might be due to a resonance-enhanced absorption originating in the aromatic ring leading to the removal of a $\pi$-electron rather than a lone pair electron from the nitrogen atom. Another possible factor governing the photoionization mass spectra of the aromatic amino acids is intramolecular charge transfer in which a charge formed initially in the functional group could transfer to the amine group or vice versa. Clearly, it is possible that this and other photochemical processes may be important here. Experiments that measure the degree of fragmentation as a function of excess energy above the ionization potential will help provide a more complete picture of which photochemical processes play a major role in these experiments. A positive sign, however, is that the α-cleavage reactions produce fragment ions that retain the identity of the parent amino acid. The potential of retaining the molecular identity through such a mechanism will be particularly valuable in surface analysis of peptides. Finally, a direct comparison of the yields obtained for photoionization of ion beam desorbed amino acids to that for SIMS has been made. We find a 2- to 8-fold increase in signal is possible for many of the amino acids and up to a 40-fold increase is possible for tyrosine.

**Acknowledgment.** This research was supported by grants from the National Institutes of Health and the National Science Foundation.

## References and Notes

(1) Wood, M.; Zhou, Y.; Brummel, C. L.; Winograd, N. *Anal. Chem.* **1994**, *66*, 2425−2432.
(2) Winograd, N. *Anal. Chem.* **1993**, *65*, 622A−629A.
(3) Pappas, D. L.; Hrubowchak, D. M.; Ervin, M. H.; Winograd, N. *Science* **1989**, *243*, 64−66.
(4) Winograd, N.; Baxter, J. P.; Kimock, F. M. *Chem. Phys. Lett.* **1982**, *88*, 581−584.
(5) Becker, C. H.; Gillen, K. T. *Appl. Phys. Lett.* **1984**, *45*, 1063−1065.
(6) Parks, J. E.; Schmitt, H. W.; Hurst, G. S.; Fairbank, W. M. *Thin Solid Films* **1983**, *108*, 69−78.
(7) Grotemeyer, J.; Schlag, E. W. *Org. Mass Spectrom.* **1988**, *23*, 388.
(8) Boesl, U.; Grotemeyer, J.; Walter, K.; Schlag, E. W. *Anal. Instrum.* **1987**, *16*, 151.
(9) Savina, M. R.; Lykke, K. R. *Trends Anal. Chem.* **1997**, *16*, 242−252.
(10) Engelke, F.; Hahn, J. H.; Henke, W.; Zare, R. N. *Anal. Chem.* **1987**, *59*, 909−912.
(11) Weinkauf, R.; Aicher, P.; Wesley, G.; Grotemeyer, J.; Schlag, E. W. *J. Phys. Chem.* **1994**, *98*, 8381−8391.
(12) Ledingham, K. W. D.; Singhal, R. P. *Int. J. Mass Spectrom. Ion Processes* **1997**, *163*, 149−168.
(13) Schütze, M.; Trappe, C.; Tabellion, M.; Kurz, H. *Fresenius' J. Anal. Chem.* **1995**, *353*, 575−577.
(14) Szaflarski, D. M.; El-Sayed, M. A. *J. Phys. Chem.* **1988**, *92*, 2234.
(15) Brummel, C. L.; Willey, K. F.; Vickerman, J. C.; Winograd, N. *Int. J. Mass Spectrom. Ion Processes* **1995**, *143*, 257−270.
(16) Willey, K. F.; Vorsa, V.; Braun, R. M.; N, W. *Rapid Commun. Mass Spectrom.* **1998**, *12*, 1253−1260.
(17) Willey, K. F.; Brummel, C. L.; Winograd, N. *Chem. Phys. Lett.* **1997**, *267*, 359−364.
(18) Möllers, R.; Terhorst, M.; Niehuis, E.; Benninghoven. *Org. Mass Spectrom.* **1992**, *27*, 1393−1395.
(19) Terhorst, M.; Möllers, R.; Niehuis, E.; Benninghoven, A. *Surf. Interface Anal.* **1992**, *18*, 824−826.
(20) Ledingham, K. W. D.; Kosmidis, C.; Georgiou, S.; Couris, S.; Singhal, R. P. *Chem. Phys. Lett.* **1995**, *247*, 555−563.
(21) Ledingham, K. W. D.; Singhal, R. P.; Smith, D. J.; McCanny, T.; Graham, P.; Kilic, H. S.; Peng, W. X.; Wang, S. L.; Langley, A. J.; Taday, P. F.; Kosmidis, C. *J. Phys. Chem. A* **1998**, *102*, 3002−3005.
(22) Smith, D. J.; Ledingham, K. W. D.; Kilic, H. S.; McCanny, T.; Peng, W. X.; Singhal, R. P.; Langley, A. J.; Taday, P. F.; Kosmidis, C. *J. Phys. Chem.* **1998**, *102*, 2519−2526.
(23) Grun, C.; Weickhardt, C.; Grotemeyer, J. *J. Eur. Mass Spectrom.* **1996**, *2*, 197−202.
(24) Benninghoven, A.; Sichtermann, W. *Anal. Chem.* **1978**, *50*, 1180−1184.
(25) Braun, R. M.; Blenkinsopp, P.; Mullock, S. J.; Corlett, C.; Willey, K. F.; Vickerman, J. C.; Winograd, N. *Rapid Commun. Mass Spectrom.* **1998**, *12*, 1246−1252.
(26) Perry, M. D.; Mourou, G. *Science* **1994**, *264*, 917−924.
(27) Backus, S.; Durfee III, C. G.; Murnane, M. M.; Kapteyn, H. C. *Rev. Sci. Instrum.* **1998**, *69*, 1207−1223.
(28) DeWitt, M. J.; Levis, R. J. *Phys. Rev. Lett.* **1998**, *81*, 5101−5104.
(29) Conjusteau, A.; Bandrauk, A. D.; Corkum, P. B. *J. Chem. Phys.* **1997**, *106*, 9095−9104.
(30) DeWitt, M. J.; Levis, R. J. *J. Chem. Phys.* **1998**, *108*, 7739−7742.
(31) DeWitt, M. J.; Levis, R. J. *J. Chem. Phys.* **1998**, *108*, 7045−7048.
(32) DeWitt, M. J.; Levis, R. J. *J. Chem. Phys.* **1995**, *102*, 8670−8673.
(33) Vorsa, V.; Willey, K. F.; Winograd, N. *Anal. Chem.* **1999**, *71*, 574−581.
(34) Keldysh, L. V. *Sov. Phys. JETP* **1965**, *20*, 1307−1314.
(35) Brown, S. B. Ultraviolet and Visible Spectroscopy. In *An Introduction to Spectroscopy for Biochemists*; Brown, S. B., Ed.; Academic Press: London, 1980; pp 14−69.
(36) McLafferty, F. W.; Turecek, F. Mass Spectra of Common Compound Classes. *Interpretation of Mass Spectra*; 4th ed.; University Science Books: Sausalito, CA, 1993; pp 225−282.
(37) Grotemeyer, J.; Walter, K.; Boesl, U.; Schlag, E. W. *Int. J. Mass Spectrom. Ion Processes* **1987**, *78*, 69−83.
(38) Weinkauf, R.; Schanen, P.; Metsala, A.; Schlag, E. W.; Bürgle, M.; Kessler, H. *J. Phys. Chem.* **1996**, *100*, 18567−18585.
(39) Holtkamp, D.; Kempken, M.; Klüsener, P.; Benninghoven, A. *J. Vac. Sci. Technol.* **1987**, *5*, 2912−2916.
(40) Benninghoven. *J. Vac. Sci. Technol.* **1985**, *A3*, 451−460.
(41) Benninghoven, A.; Lange, W.; Jirikowsky, M.; Holtkamp, D. *Surf. Sci. Lett.* **1982**, *123*, L721−L727.
(42) Benninghoven, A.; Jaspers, D.; Sichtermann, W. *Appl. Phys.* **1976**, *11*, 35−39.
(43) Van Vaeck, L.; Van Roy, W.; Gijbels, R.; Adams, F. Structural Characterization of Organic Molecules by laser Mass Spectrometry. In *Laser Ionization Mass Ananlysis*; Vertes, A., Gijbels, R., Adams, F., Eds.; John Wiley & Sons: New York, 1993; Vol. 124, pp 150−152.
(44) Parker, C. D.; Hercules, D. M. *Anal. Chem.* **1986**, *58*, 25−30.
(45) Parker, C. D.; Hercules, D. M. *Anal. Chem.* **1985**, *57*, 698−704.
(46) Hillenkamp, F.; Karas, M.; Holtkamp, D.; Klüsener, P. *Int. J. Mass Spectrom. Ion Processes* **1986**, *69*, 265−276.
(47) Schiller, C.; Kupka, K.-D.; Hillenkamp, F. *Fresenius' Z. Anal. Chem.* **1981**, *308*, 304−308.
(48) Campbell, S.; Beauchamp, J. L.; Rempe, M.; Lichtenberger, D. L. *Int. J. Mass Spectrom. Ion Processes* **1992**, *117*, 83−99.